On the stratospheric aerosol budget at Northern mid-latitudes from 22 years of ground-based lidar and satellite observations

S. Khaykin[1], S. Godin-Beekmann[1], P. Keckhut[1], A. Hauchecorne[1], J.-P. Vernier[2,3], A. Bourassa[4], C. Bingen[5], M. DeLand[6], P.K. Bhartia[6]

1 LATMOS/IPSL, UVSQ Université Paris-Saclay, UPMC Univ. Paris 06, CNRS, Guyancourt, France.
2 Science Systems and Applications, Inc., Hampton, Virginia, US.
3 NASA Langley Research Center, Hampton, Virginia, US.
4 Institute of Space and Atmospheric Science, University of Saskatchewan, Saskatoon, Saskatchewan, Canada.
5 Royal Belgian Institute for Space Aeronomy, Brussels, Belgium
6 Science Systems and Applications, Inc., Lanham, Maryland, USA

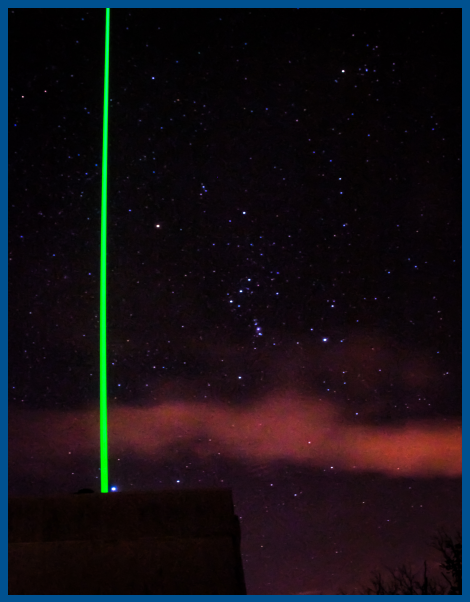

SSiRC, 25-28 April, Potsdam

Motivation

- Stratospheric aerosol load at quasi-background level after 1998 with several transient perturbations due to VEI 4 eruptions
- Opportunity for investigation of non-volcanic aerosol drivers and its long-term change
- Remote detection of small aerosol abundances is challenging

=> **Combination of data sets** required for accurate characterization of background stratospheric aerosol variability

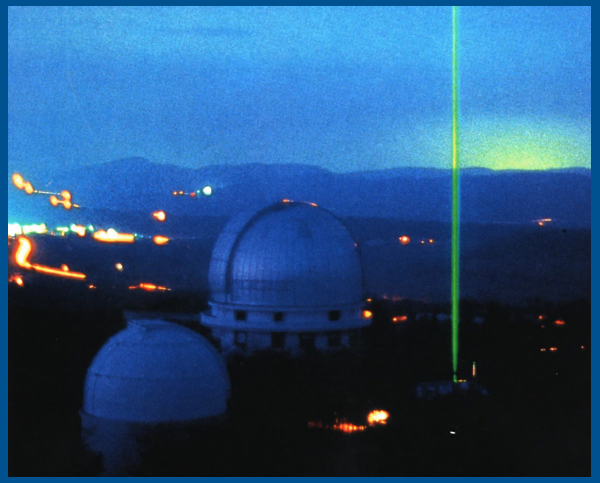

OHP lidars: specs and aerosol retrieval

⇒ Use of powerful ozone DIAL (LiO3S) and temperature (LTA) NDACC lidars for stratospheric aerosol retrieval (Z > 13 km)

⇒ Brand-new stratospheric aerosol data set spanning 1994-present

LiO3S (ozone DIAL)	LTA (Rayleigh-Mie-Raman)
• Nd:YAG laser, 2.4 W	• Nd:YAG laser, 15 W (24 W after 2013)
• off-line **355 nm** channel	• **532 nm** emission/reception
• 0.88 m^2 mosaic telescope	• Low gain channel (0.031 m^2 telescope)
• 3118 acquisition nights	• 2691 acquisition nights
• 17 % rejection rate	• 11 % rejection rate
• 9 profiles per month on average	• 10 profiles per month on average
• Godin-Beekmann et al., 2003	• Hauchecorne et al, 1992

- Fernald-Klett inversion
- Lidar ratio and Angstrom exponents from Jäger and Deshler (2002; 2003)
- Molecular backscatter from daily NCEP meteorological data
- Reference (zero-aerosol) altitude between 30 .. 33 km

OHP lidars: observations

Stratospheric Aerosol Optical Depth 17-30 km ($sAOD_{1730}$) @ 532 nm

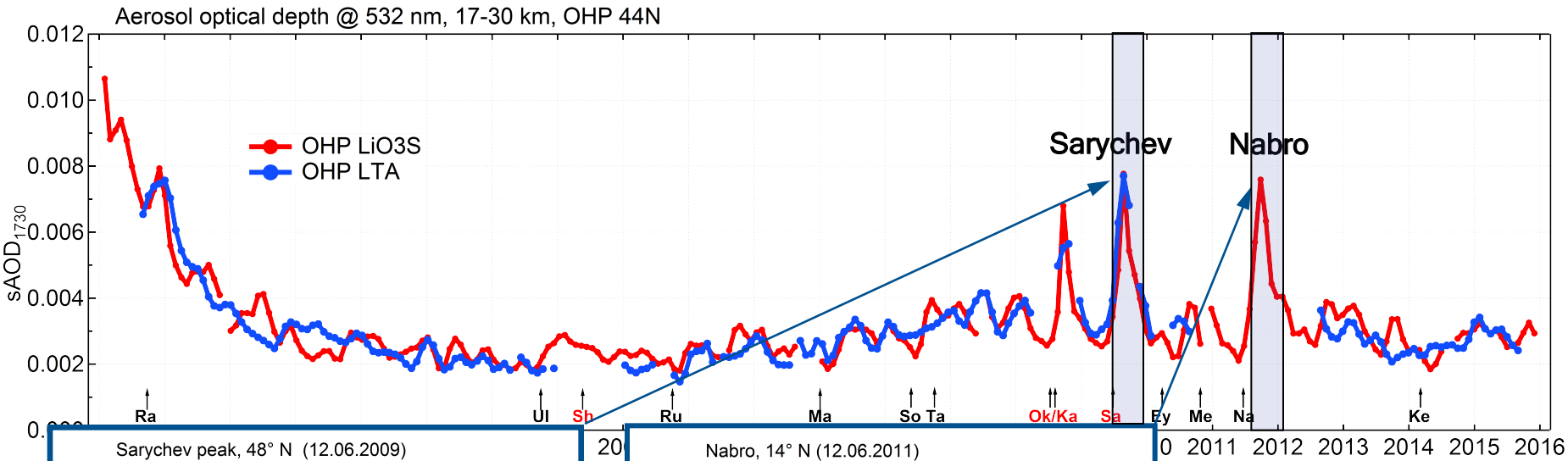

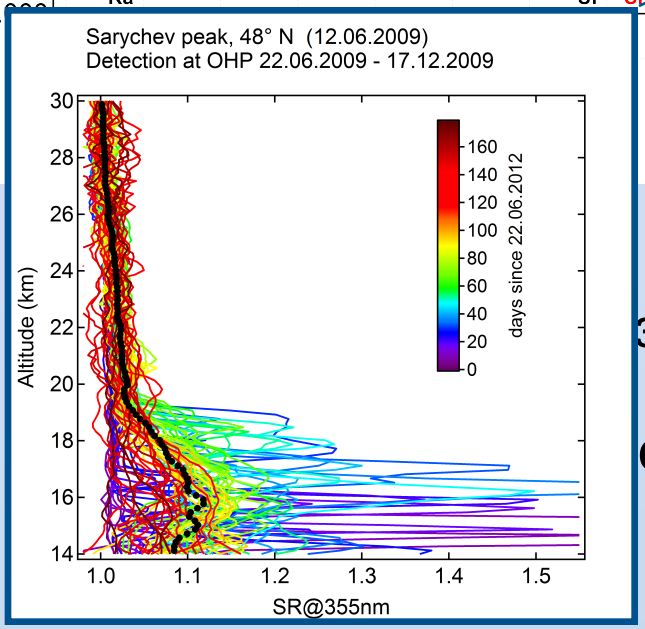

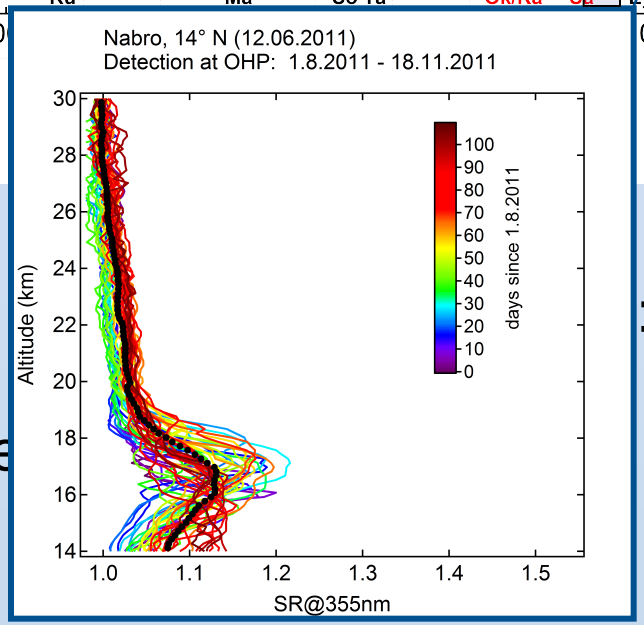

OHP lidars and satellites: sAOD comparison

Stratospheric Aerosol Optical Depth 17-30 km ($sAOD_{1730}$) @ 532 nm

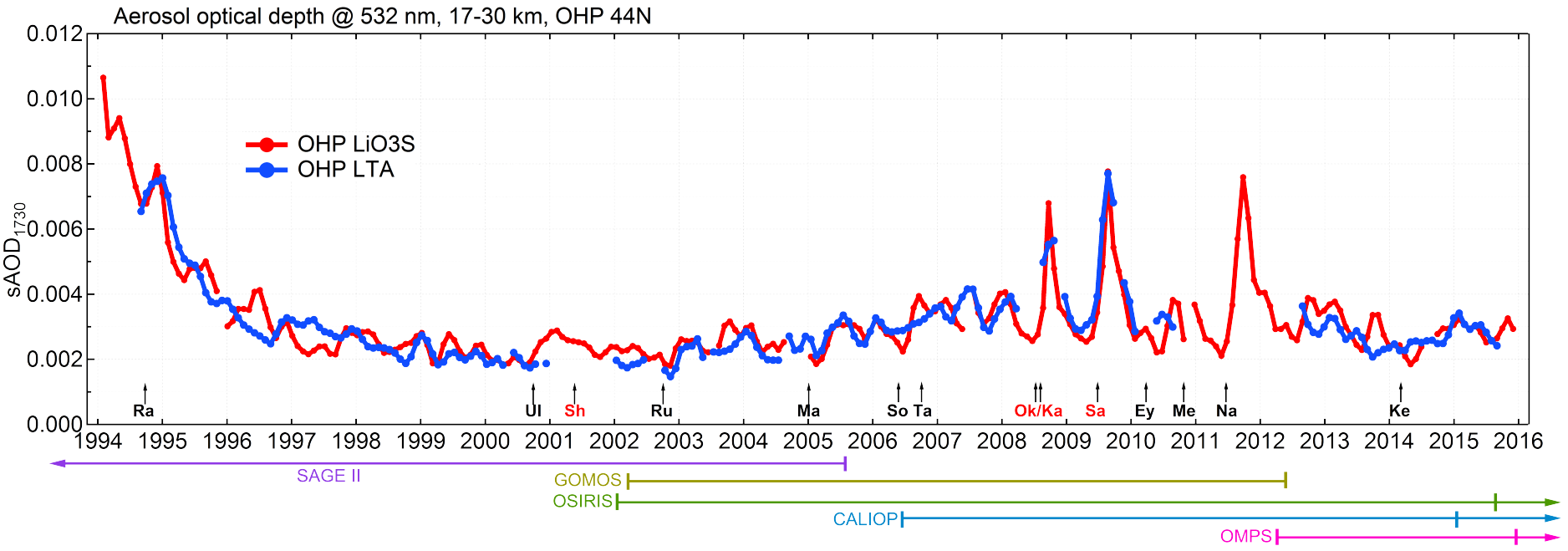

LiO3S 355 nm (*ke*=1.6 ater 1997)
LTA 532 nm

SAGE II 525 nm (*ke*=1.6 ater 1997)
GOMOS 550 nm (*ke*=1.6)
OSIRIS 750 nm (*ke*=2.0)
CALIOP 532 nm
OMPS 675 nm (*ke*=1.8)

All converted to 532 nm

OHP lidars and satellites: sAOD comparison

Stratospheric Aerosol Optical Depth 17-30 km ($sAOD_{1730}$) @ 532 nm

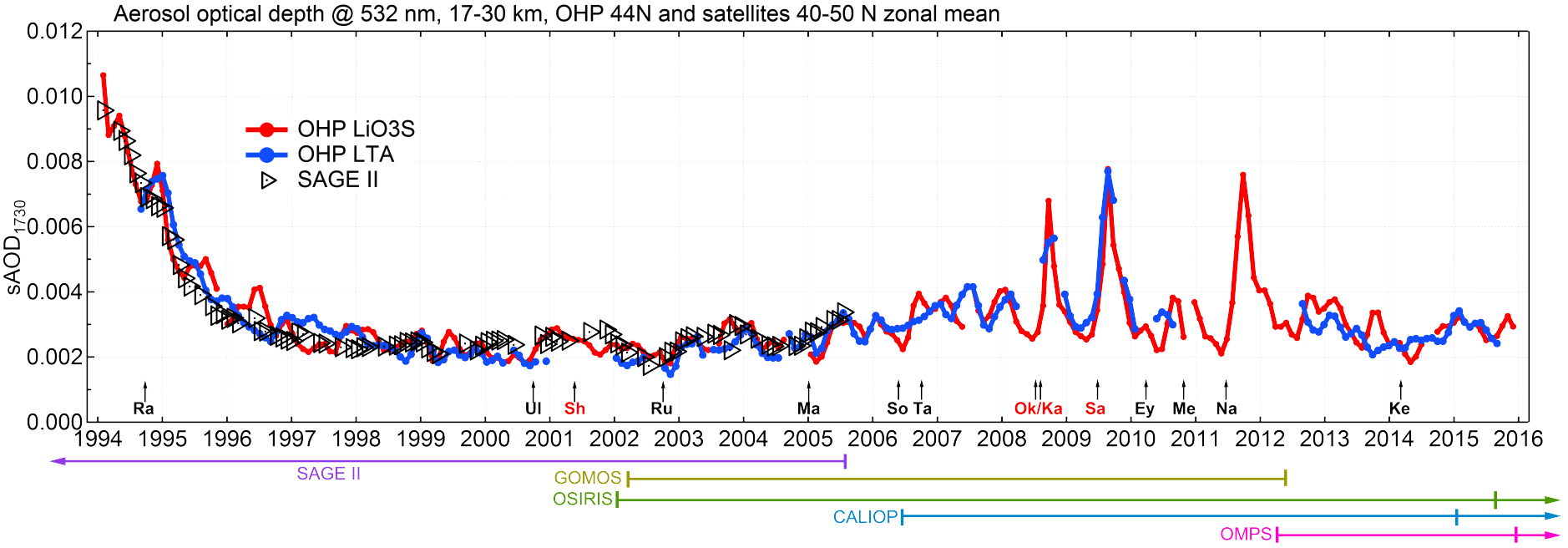

OHP lidars vs SAGE II

	Mean rel. diff (%) ± 2 standard errors	Correlation coef. R
LiO3S	2.1 ± 3.3	0.97
LTA	-2.1 ± 4.4	0.96

OHP lidars and satellites: sAOD comparison

Stratospheric Aerosol Optical Depth 17-30 km ($sAOD_{1730}$) @ 532 nm

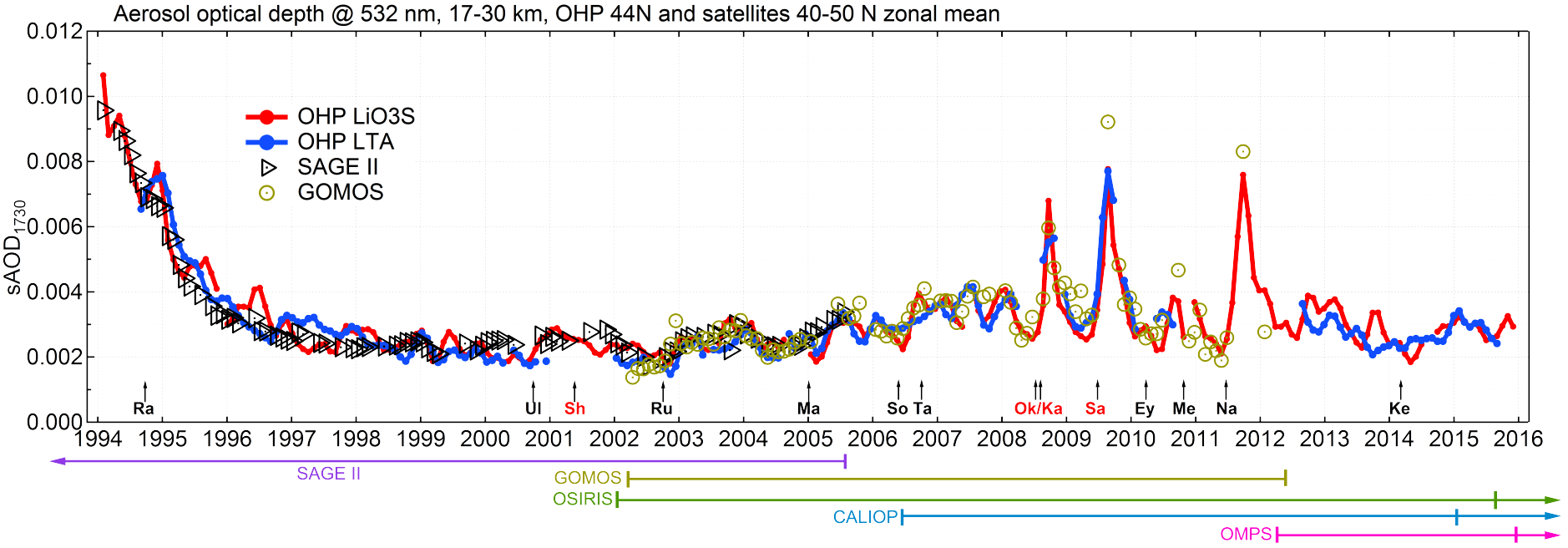

OHP lidars vs GOMOS (AerGOM)

	Mean rel. diff (%) ± 2 standard errors	Correlation coef. R
LiO3S	0.4 ± 4.0	0.9
LTA	-2.9 ± 4.3	0.86

OHP lidars and satellites: sAOD comparison

Stratospheric Aerosol Optical Depth 17-30 km ($sAOD_{1730}$) @ 532 nm

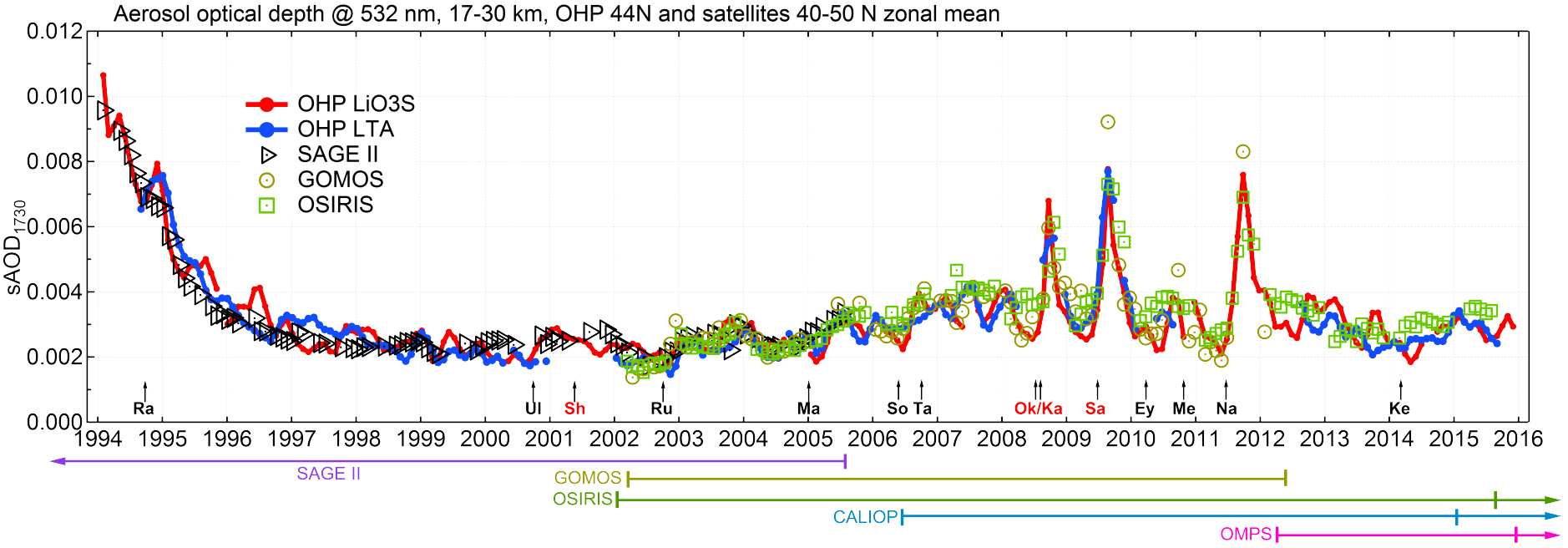

OHP lidars vs OSIRIS V5.7 (ke=2.0)

	Mean rel. diff (%) ± 2 standard errors	Correlation coef. R
LiO3S	-6.6 ± 3.4	0.81
LTA	-7.4 ± 2.7	0.9

OHP lidars and satellites: sAOD comparison

Stratospheric Aerosol Optical Depth 17-30 km ($sAOD_{1730}$) @ 532 nm

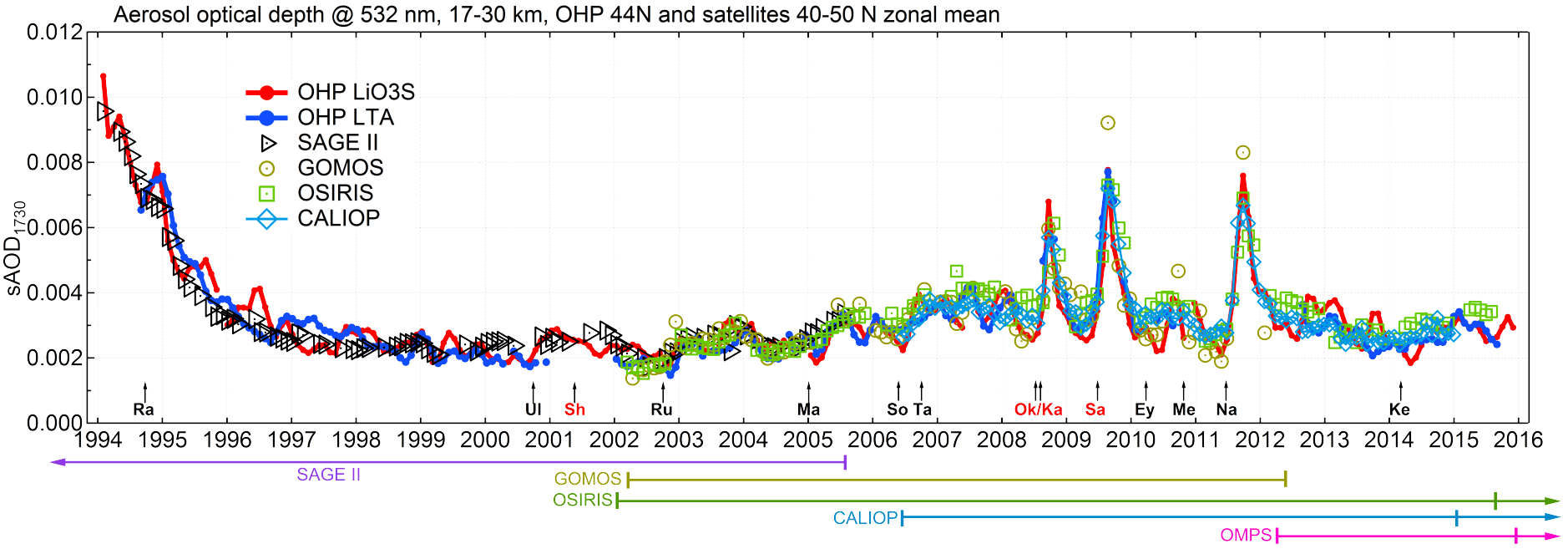

OHP lidars vs CALIOP V4 (lidar ratio = 50 sr)

	Mean rel. diff (%) ± 2 standard errors	Correlation coef. R
LiO3S	-2.2 ± 3.4	0.85
LTA	-0.4 ± 2.5	0.94

OHP lidars and satellites: sAOD comparison

Stratospheric Aerosol Optical Depth 17-30 km ($sAOD_{1730}$) @ 532 nm

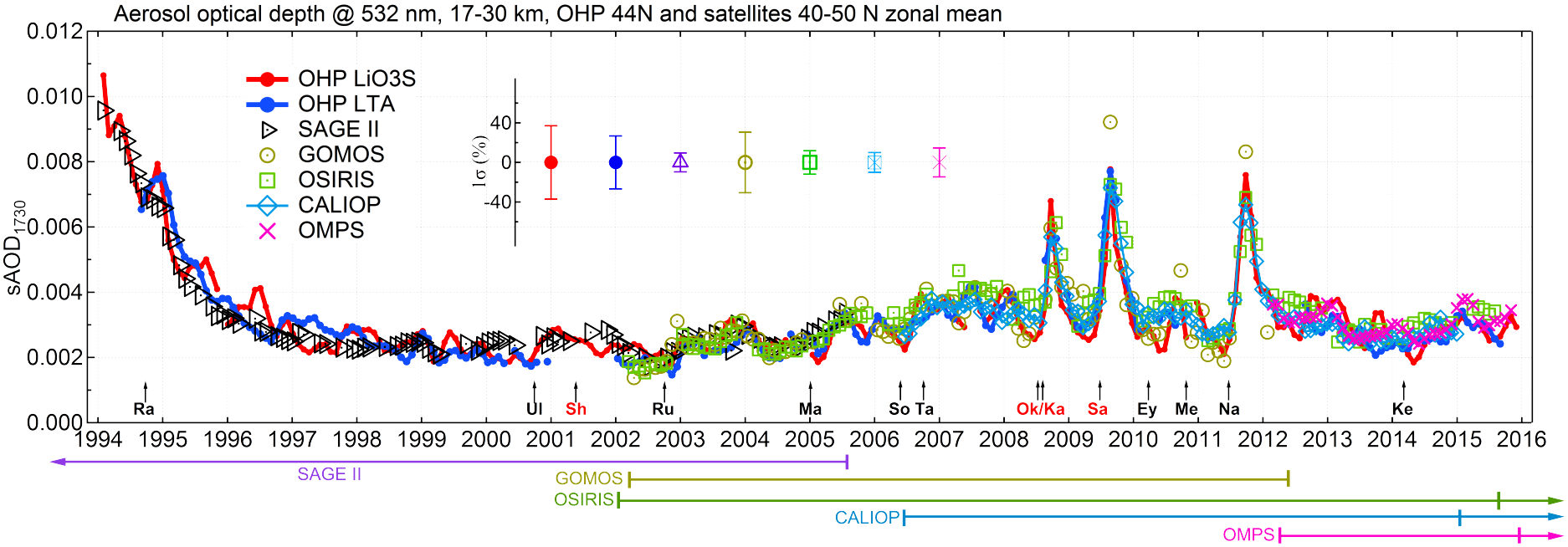

LiO3S 355 nm (*ke*=1.6 ater 1997)
LTA 532 nm

SAGE II 525 nm (*ke*=1.6 ater 1997)
GOMOS 550 nm (*ke*=1.6)
OSIRIS 750 nm (*ke*=2.0)
CALIOP 532 nm
OMPS 675 nm (*ke*=1.8)

All converted to 532 nm

OHP lidars and satellites

Stratospheric Aerosol Optical Depth 17-30 km ($sAOD_{1730}$) @ 532 nm

Mean of OHP lidars and satellites

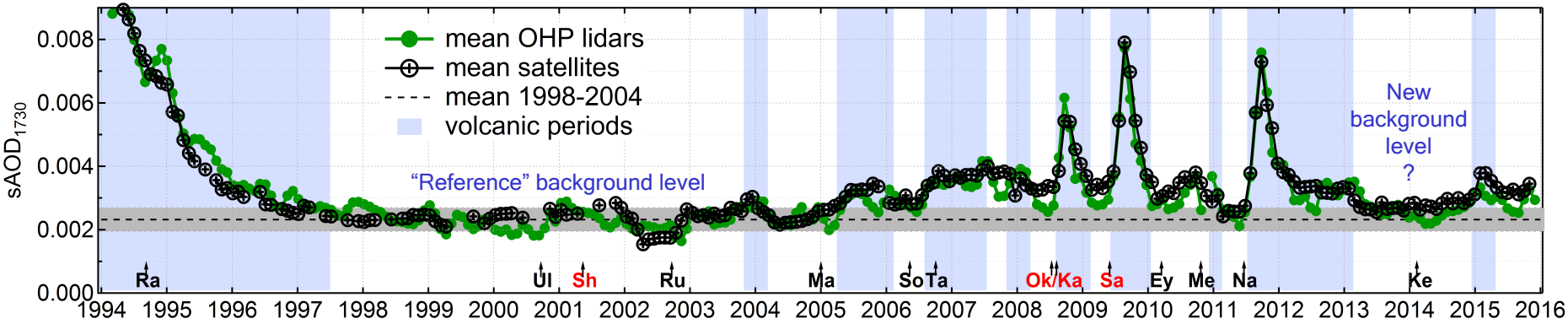

- Volcanically-perturbed periods identified using satellite global-coverage
- "Reference" background level of sAOD at mid-latitudes accurately determined
- New background level ?

AOD within 15-19 km from CALIOP and OHP-LiO3S

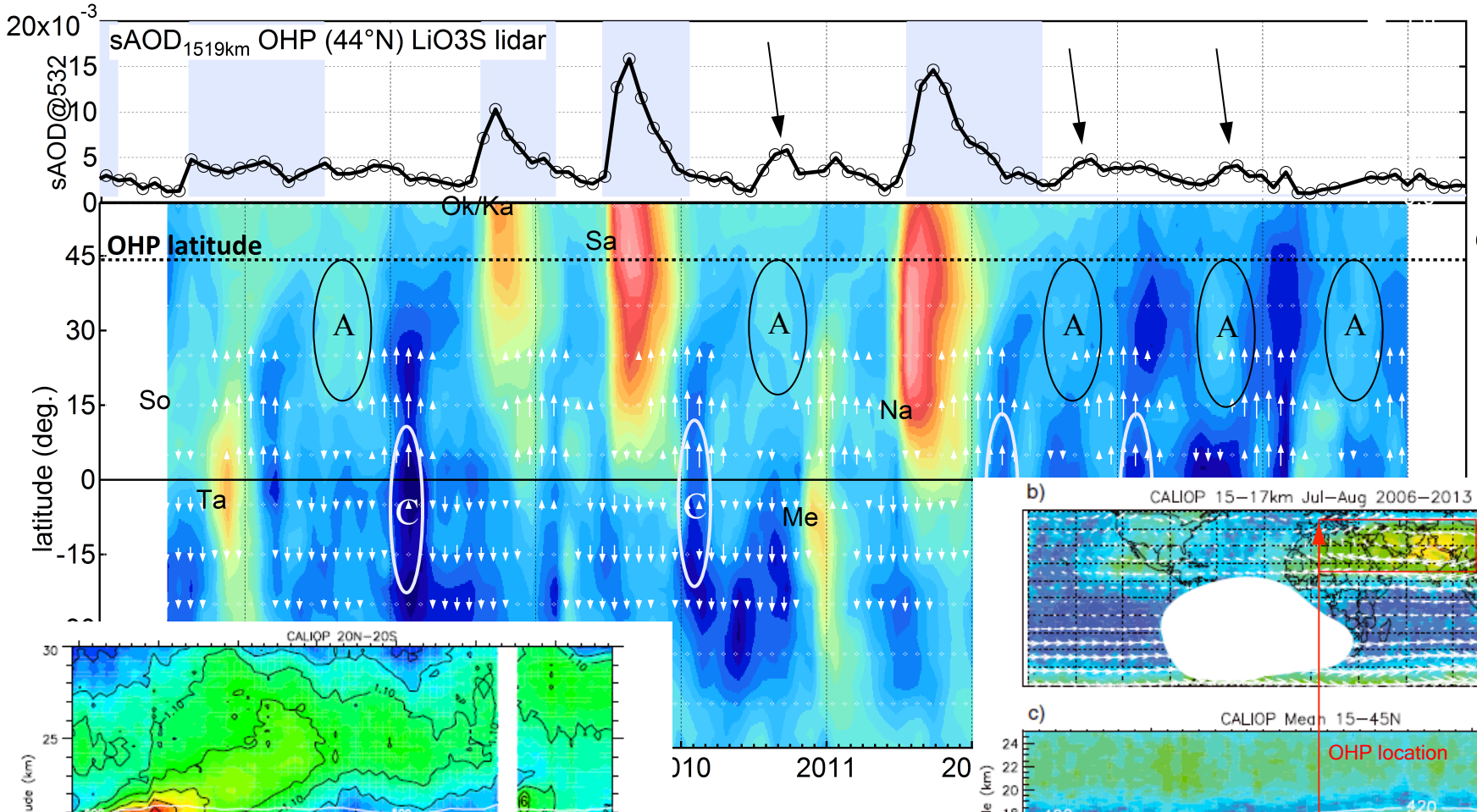

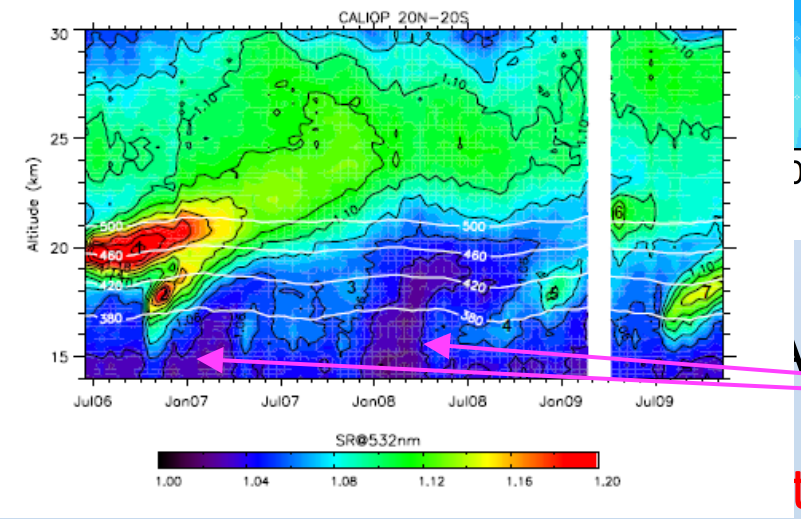

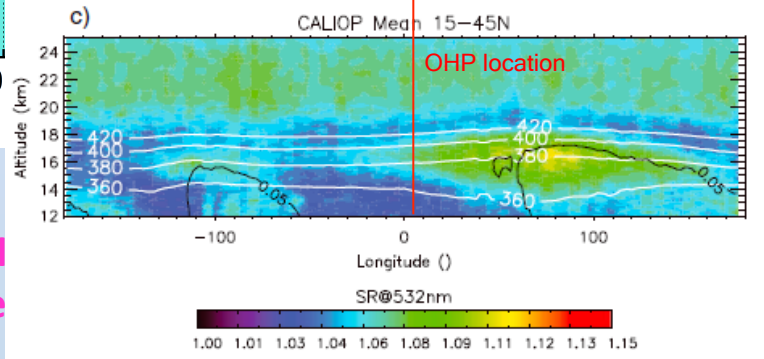

Aerosol Layer)

Overshooting of cl
tropical LS (Vernie

times since 1997 (Vernier et al., 2015)

Annual cycle of aerosol scattering ratio

OHP lidar : entire period

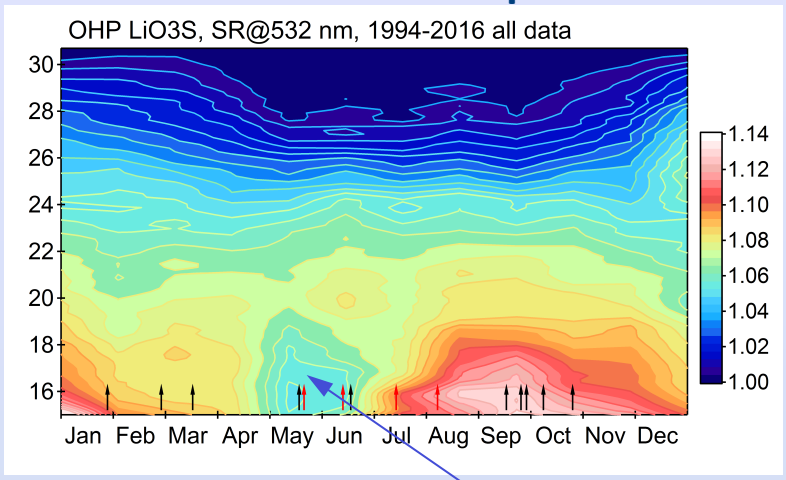

OHP lidar : volcanoes cleared

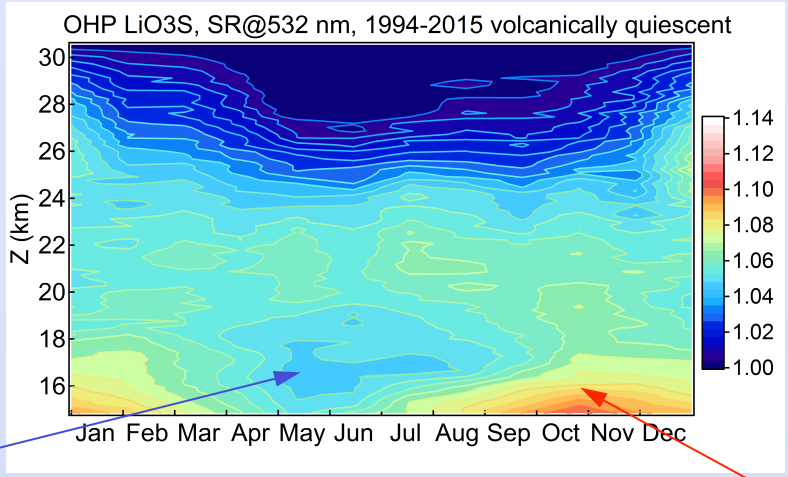

Clean and dry LS feature in late spring

Influx of aerosol-rich and humid air from Asian monsoon

CALIOP: 40-50°N volcanoes cleared

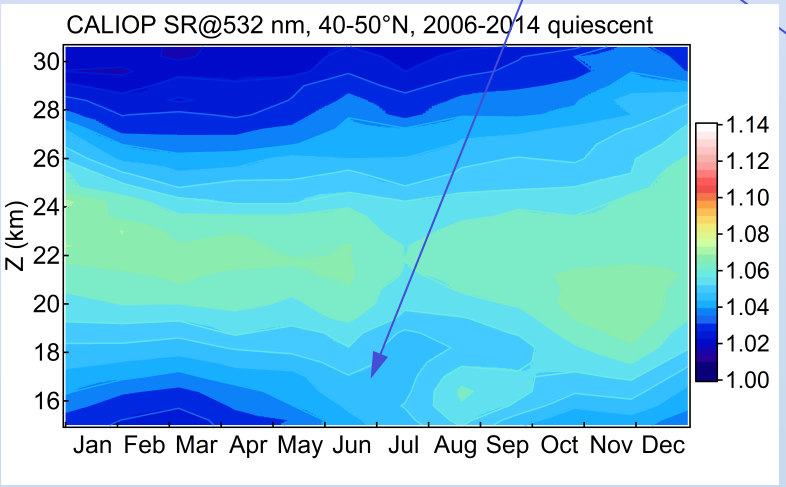

MLS H_2O: 40-50°N 2006-2014

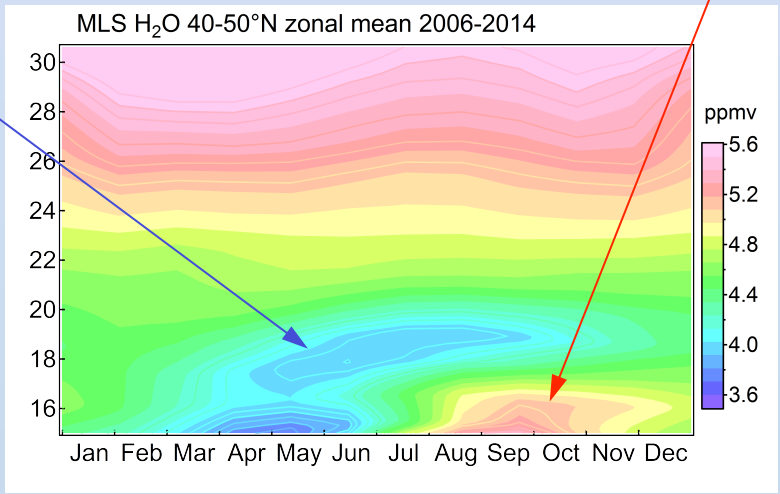

Aerosol and water vapour

CALIOP AOD_{1519}

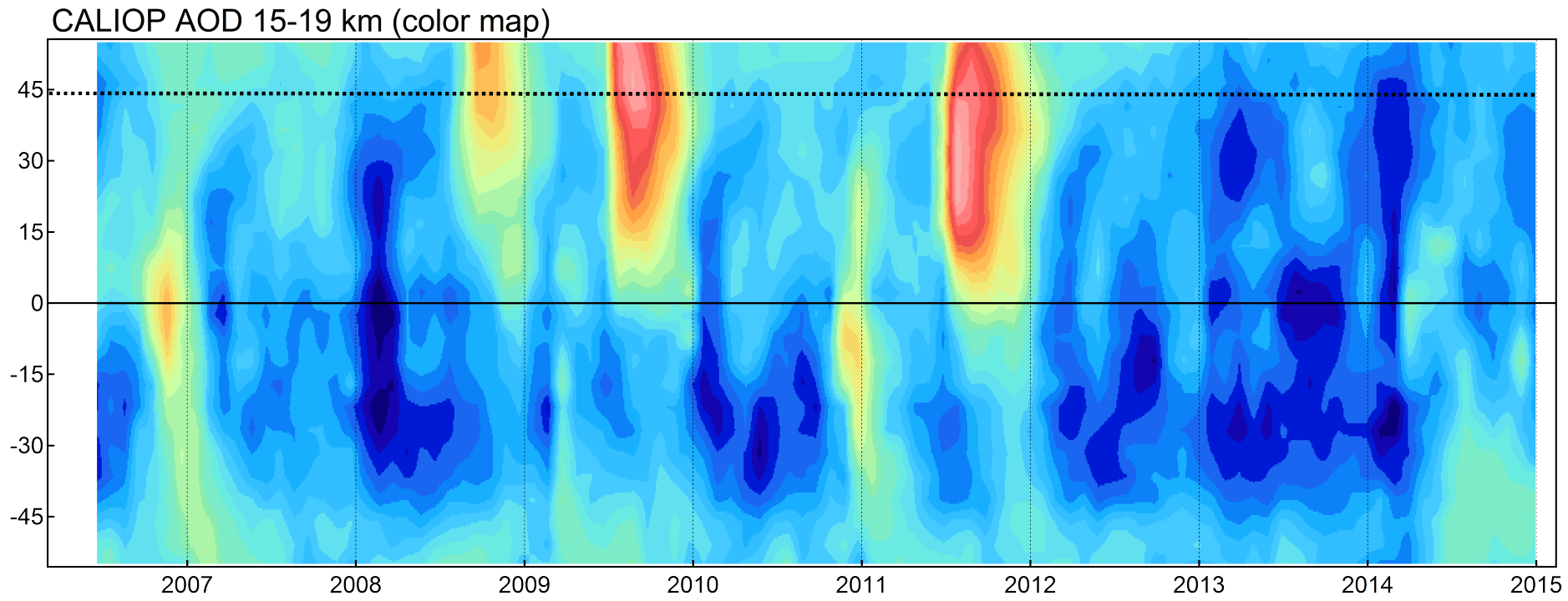

Aerosol and water vapour

CALIOP AOD_{1519} + MLS H_2O @ 100 hPa

Contours = dry air

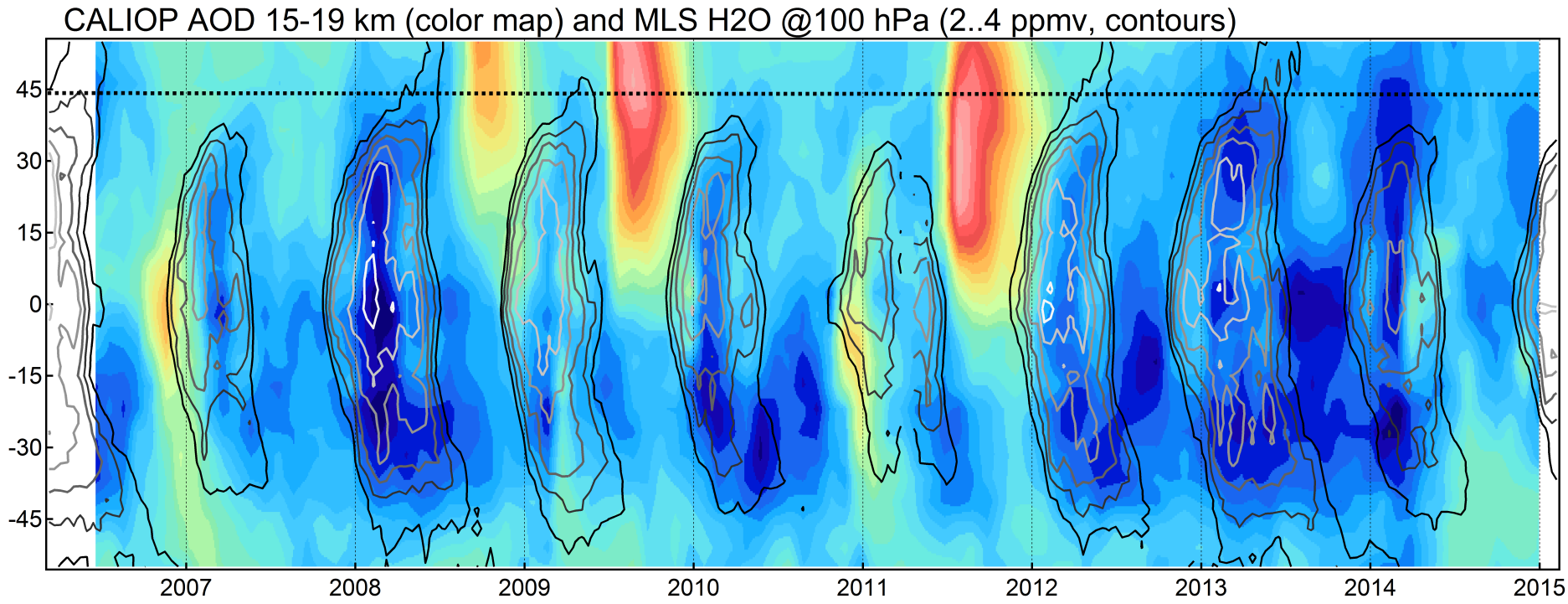

Aerosol and water vapour

CALIOP AOD_{1519} + MLS H_2O @ 100 hPa

Contours = humid air

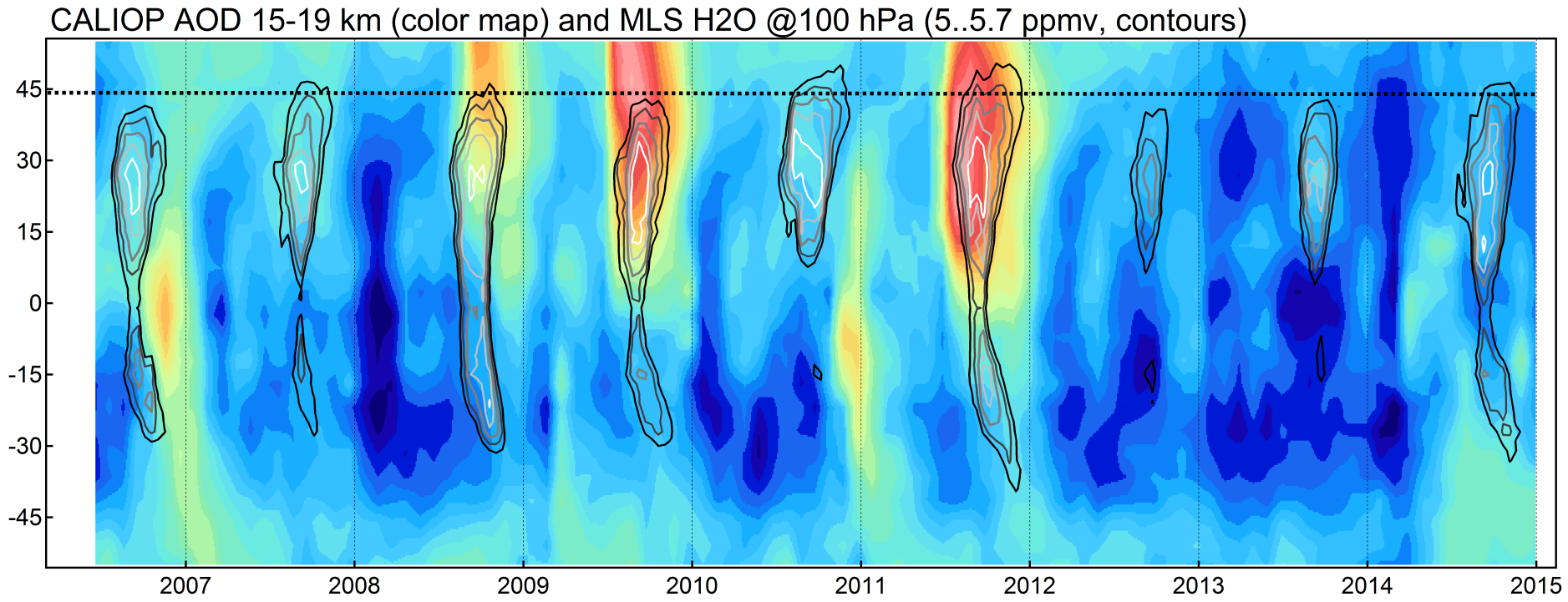

Aerosol annual cycle and long-term change

Background aerosol annual cycle

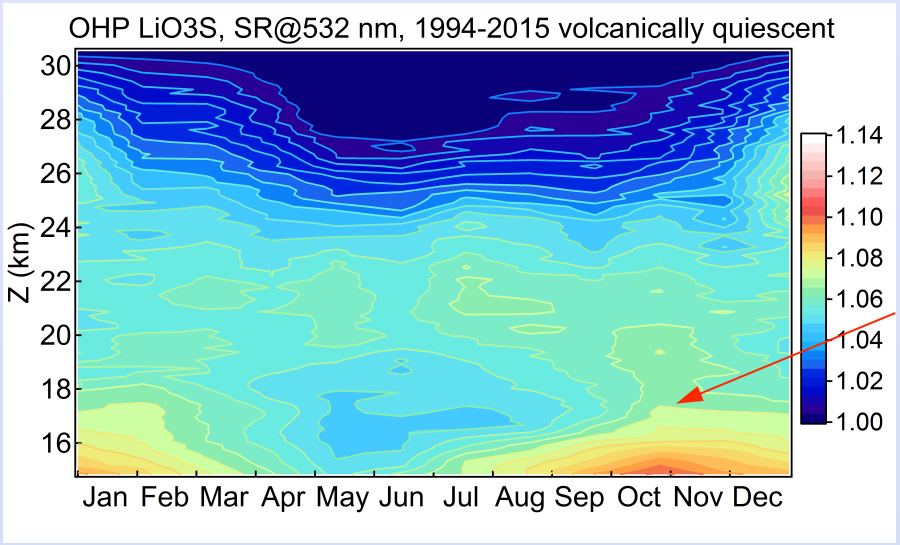

Pollut

Summer/winter ratio of AOD 13-18 km above Eastern Mediterranean

Vernier et al., 2015

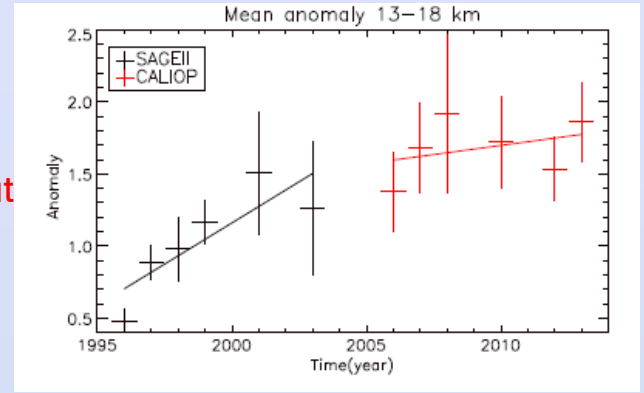

Background aerosol long-term change

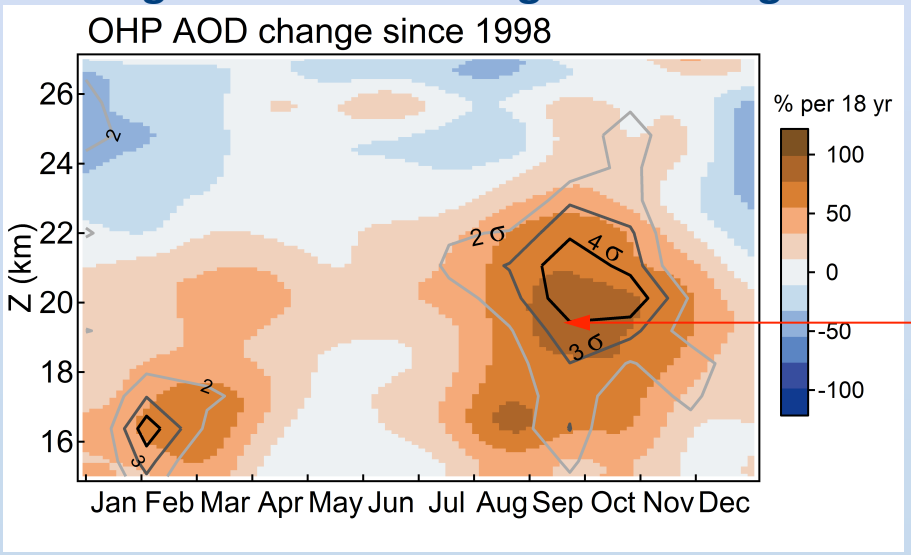

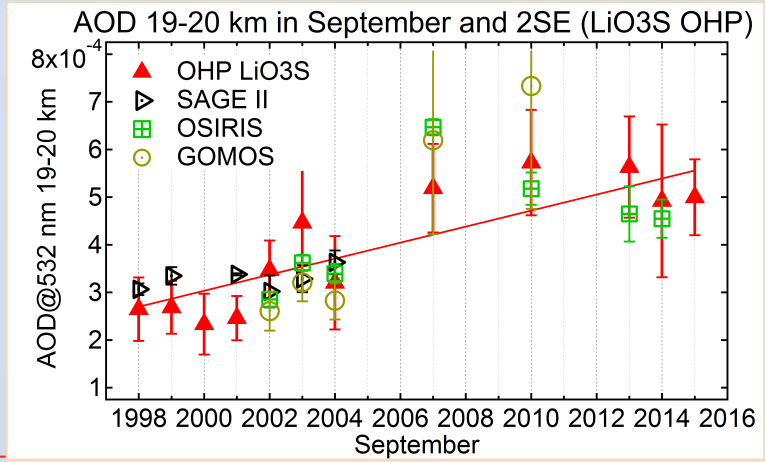

Statistically significant 2 times increase of LS AOD in early Fall

Reason for sAOD increase of 15% since the previous quiescent period?

Summary

- ✓ New high-quality stratospheric aerosol data set from OHP lidars

- ✓ Combination of GB lidars and satellites allows for careful examination of background mid-latitude stratospheric aerosol drivers and evolution

- ✓ Annual cycle of mid-latitude background aerosol is driven by remote (tropical) processes followed by poleward transport:
  - i) Overshooting of clean air during Austral summer
  - ii) Uplift of polluted air within the Asian monsoon during Boreal summer

- ✓ Doubling of LS AOD since 1998 in early Fall associated with growing ATAL optical depth

Supporting slides

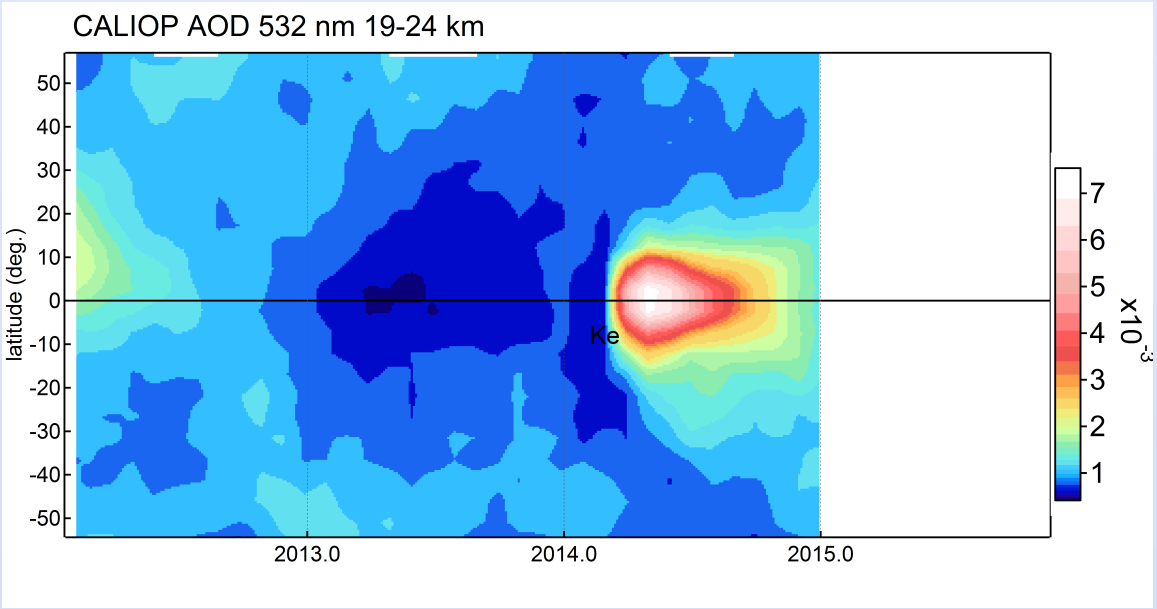

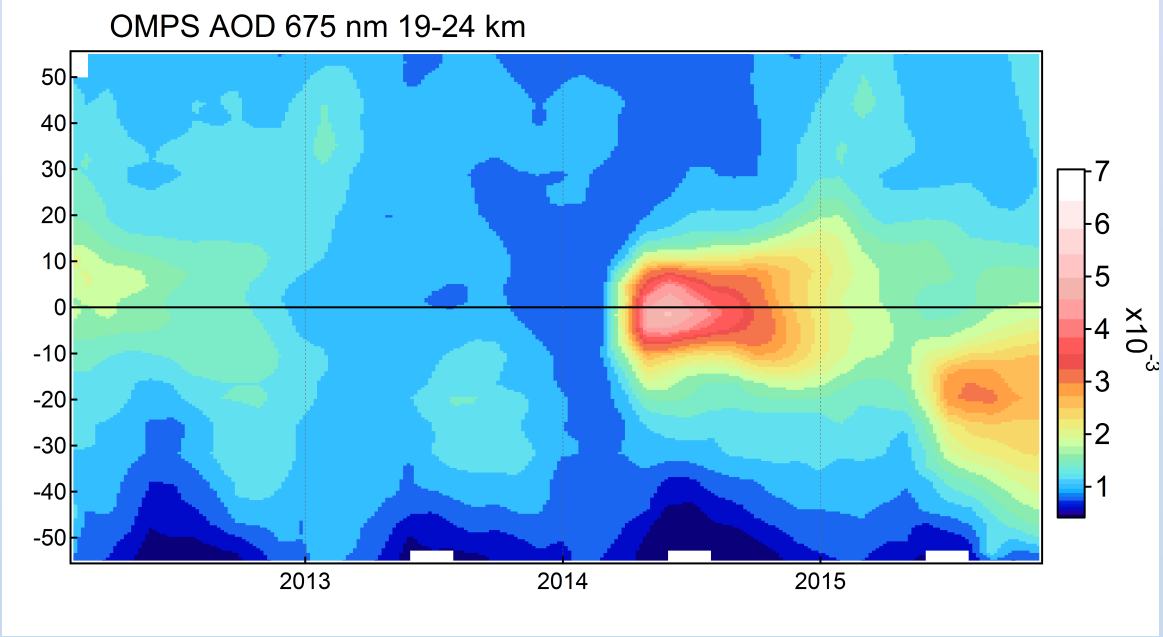

Supporting slides

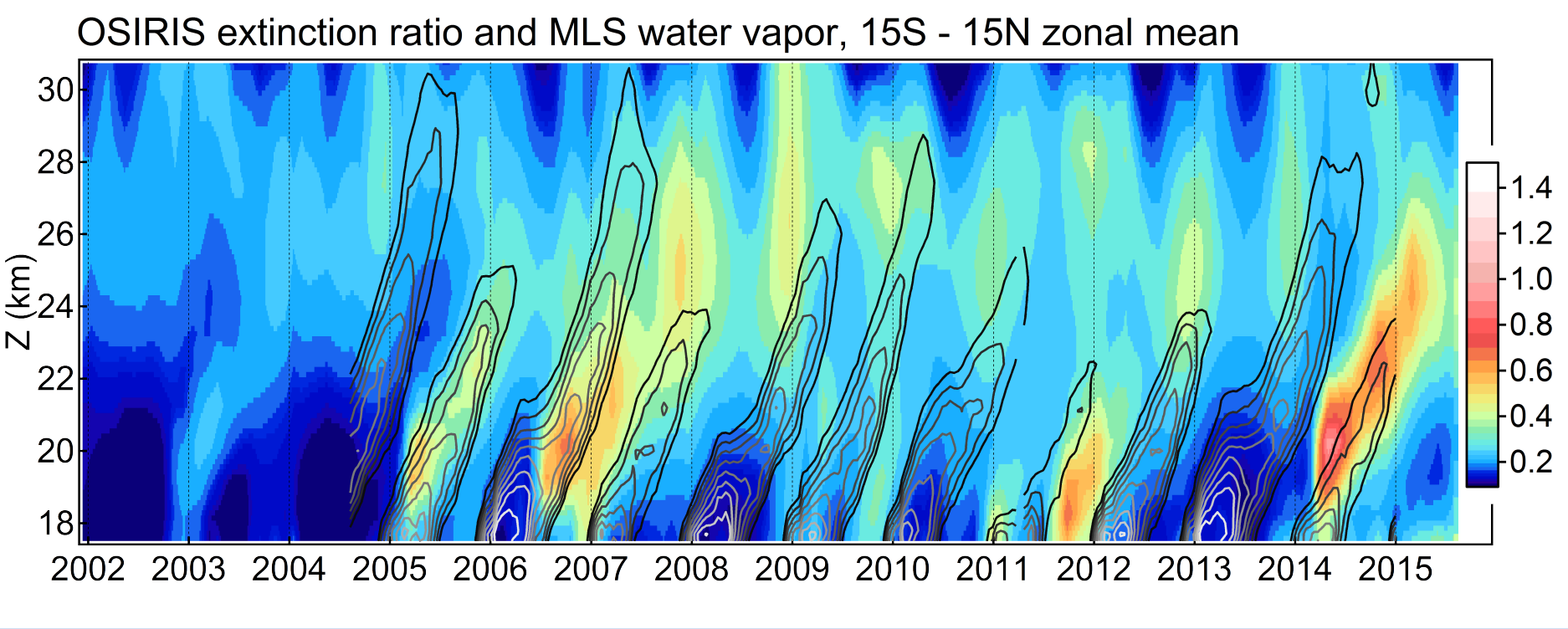

Supporting slides

Intercomparison of stratospheric Aerosol Optical Depth between 17 and 30 km (sAOD1730) series. Mean relative difference Δ_{mean} ± 2 standard errors

Δ_{mean} ± 2SE, %	LiO3S	LTA	SAGE II	GOMOS	OSIRIS	CALIOP	OMPS	Sat_mean
LiO3S		0.65 ± 2.4	2.1 ± 3.3	0.4 ± 4.0	-6.6 ± 3.4	-2.2 ± 3.4	-4.8 ± 4.3	-1.5 ± 2.2
LTA			-2.1 ± 4.4	-2.9 ± 4.3	-7.4 ± 2.7	-0.4 ± 2.5	-8.6 ± 3.3	-2.7 ± 2.1
SAGE II				-0.1 ± 5.9	7.7 ± 6.0			2.1 ± 2.7
GOMOS					-5.8 ± 3.4	-1.6 ± 3.7		-1.9 ± 1.9
OSIRIS						7.8 ± 2.5	6.6 ± 4.0	3.2 ± 1.3
CALIOP							-5.6 ± 3.4	-3.1 ± 1.2

Supporting slides

Intercomparison of stratospheric Aerosol Optical Depth between 17 and 30 km (sAOD1730) series. Correlation coefficient R

R correl	LiO3S	LTA	SAGE II	GOMOS	OSIRIS	CALIOP	OMPS	Sat_mean
LiO3S		0.9	0.97	0.9	0.81	0.85	0.63	0.94
LTA			0.96	0.86	0.9	0.94	0.66	0.94
SAGE II				0.7	0.85	-	-	
GOMOS					0.86	0.88		
OSIRIS						0.93	0.65	
CALIOP							0.71	

Supporting slides

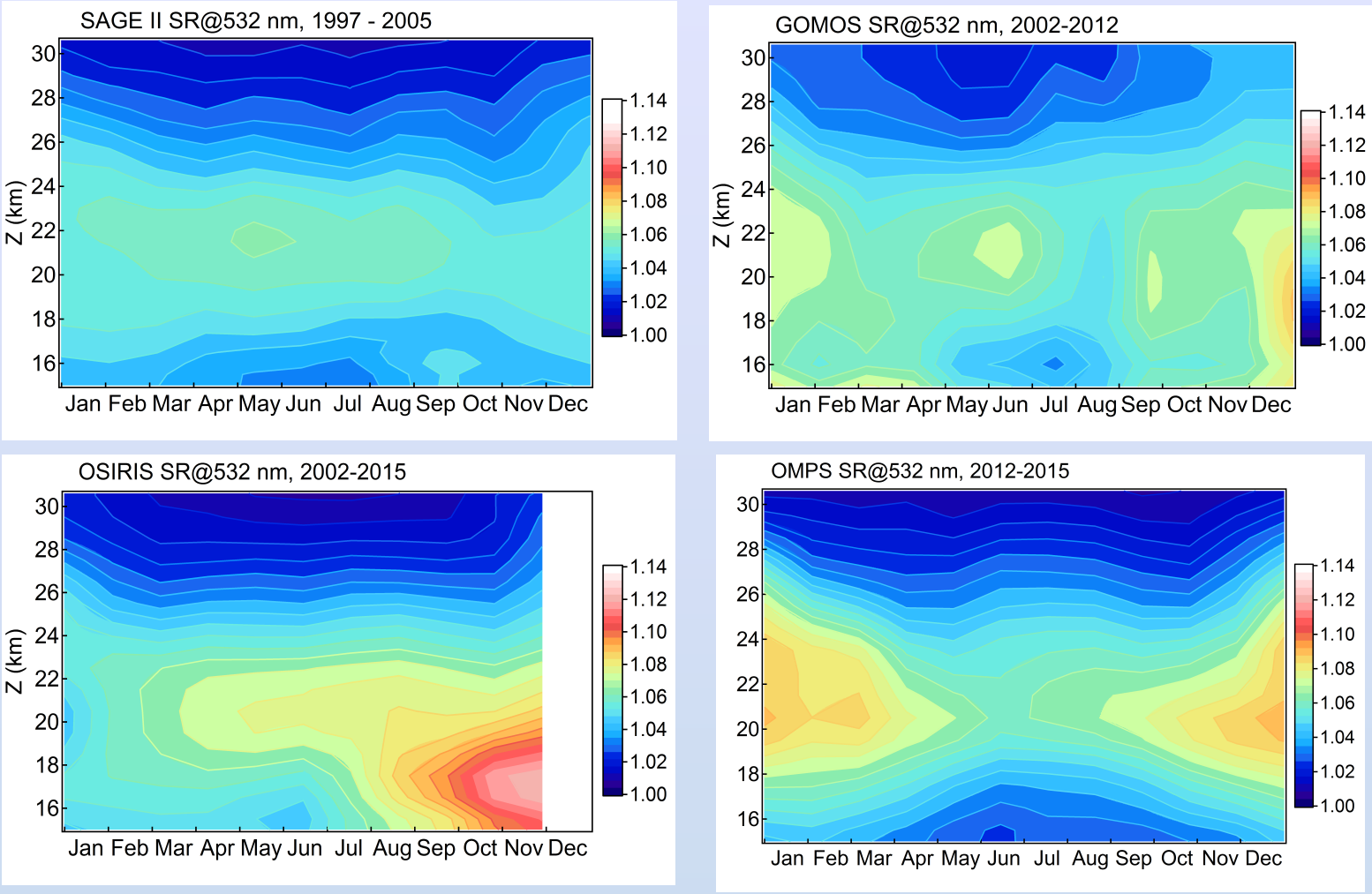

Figure S2. Month-altitude sections of aerosol scattering ratio from SAGE II, GOMOS, OSIRIS and OMPS/LP for the available observation period of each satellite instrument as denoted in each panel. The late spring minimum and its upward propagation, associated with influx of clean air from the

Supporting slides

Vertically-resolved scattering ratio series from 2 lidars

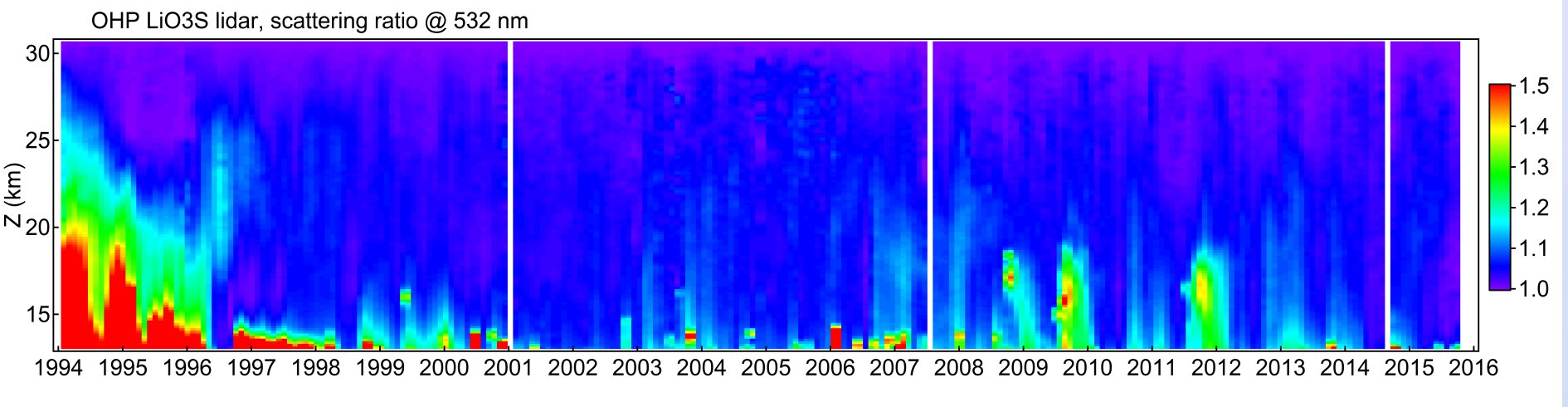

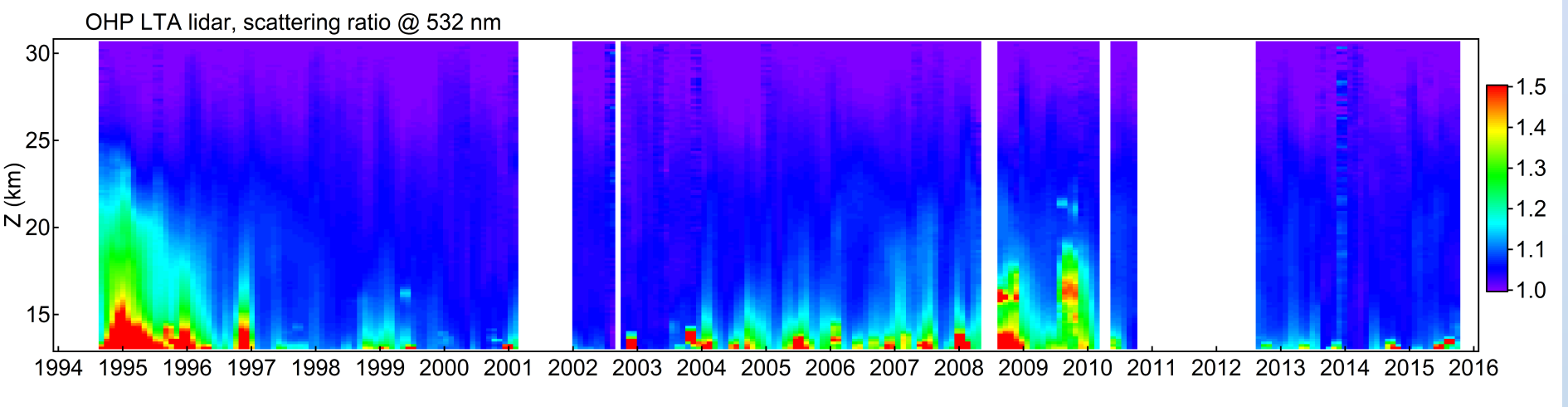

Supporting slides

OHP lidars vs OMPS/LP V0.5 (ke=1.8)

	Mean rel. diff (%) ± 2 standard errors	Correlation coef. R
LiO3S	-4.8 ± 4.3	0.63
LTA	-8.6 ± 3.3	0.66

Supporting slides

NDACC aerosol lidars at NH mid-latitudes lack consistency